Published online December 15, 2004

Nucleic Acids Research, 2004, Vol. 32, No. 22 ***6595–6604***
doi:10.1093/nar/gkh998

Peptide conjugates for chromosomal gene targeting by triplex-forming oligonucleotides

Faye A. Rogers[1,2], Muthiah Manoharan[3], Peter Rabinovitch[2], David C. Ward[2] and Peter M. Glazer[1,2,*]

[1]Department of Therapeutic Radiology and [2]Department of Genetics, Yale University School of Medicine, 295 Congress Avenue, New Haven, CT 068520, USA and [3]Isis Pharmaceuticals, Carlsbad, CA, USA

Received September 30, 2004; Revised and Accepted November 24, 2004

ABSTRACT

Triplex-forming oligonucleotides (TFOs) are DNA-binding molecules, which offer the potential to selectively modulate gene expression. However, the biological activity of TFOs as potential antigene compounds has been limited by cellular uptake. Here, we investigate the effect of cell-penetrating peptides on the biological activity of TFOs as measured in an assay for gene-targeted mutagenesis. Using the transport peptide derived from the third helix of the homeodomain of antennapedia (Antp), we tested TFO–peptide conjugates compared with unmodified TFOs. TFOs covalently linked to Antp resulted in a 20-fold increase in mutation frequency when compared with 'naked' oligonucleotides. There was no increase above background in mutation frequency when Antp by itself was added to the cells or when Antp was linked to mixed or scrambled sequence control oligonucleotides. In addition, the TFO–peptide conjugates increased the mutation frequency of the target gene, and not the control gene, in a dose-responsive manner. Confocal microscopy using labeled oligonucleotides indicated increased cellular uptake of TFOs when linked to Antp, consistent with the gene-targeting data. These results suggest that peptide conjugation may enhance intranuclear delivery of reagents designed to bind to chromosomal DNA.

INTRODUCTION

Triplex-forming oligonucleotides (TFOs) are molecules that bind in a sequence specific manner to duplex DNA. TFOs are attractive candidates for use in genetic manipulation and are poised for development into gene-based therapeutics. TFOs bind as third strands in the major groove of duplex DNA at polypurine/polypyrimidine stretches (1,2). Their specificity arises from the base triplets formed either by Hoogsteen or reverse Hoogsteen hydrogen bonds between the third strand and the purine strand of the duplex. TFOs have been successfully used to inhibit transcription (3), damage DNA through delivery of a mutagen (4–7) and provoke mutagenesis through high-affinity binding (8,9). Triplex formation has also been shown to stimulate recombination in mammalian cells in both episomal and chromosomal targets (10–12).

Although TFOs are promising reagents for gene targeting, one of the biggest challenges in their application as potential therapeutic agents is efficient delivery into the targeted cells both in animal and cell culture models. While most mammalian cells appear to be capable of internalizing oligonucleotides, simple addition to cell culture medium does not efficiently achieve the concentration required for pharmacologic effect. Because oligonucleotides are relatively large and polyanionic, their uptake by passive diffusion is limited. In fact, it has been shown that oligonucleotides are mostly taken up by cells via endocytosis (13). Therefore, a large portion of the oligonucleotides becomes trapped in the endosomes, resulting in nuclease-mediated degradation, with relatively little intact oligonucleotide released into the cytoplasm.

Both cellular uptake and intracellular compartmentalization need to be improved to increase the efficacy of TFOs. As such, research has focused on the design of useful and efficient methods for the delivery of nucleic acids into cells. Presently, the most commonly used techniques include microinjection, co-mixture with cationic liposomes and electroporation (14–17). However, these techniques are characterized by a series of limitations including cytotoxicity and induced stress on the cell. Although oligonucleotide delivery via cationic lipids is commonly used, it has been known to be sensitive to serum, antibiotics and certain cell culture medium. One set of experiments has shown that microinjection of TFOs into cells can substantially increase their biological effect, as measured by induced recombination (11). These experiments served to demonstrate the importance of delivery in determining the efficacy of gene-targeting reagents. However, the technical difficulty of microinjection prevents its widespread application.

An attractive strategy, with theoretically fewer drawbacks, is to link oligonucleotides to certain peptides which are able to pass through cell membranes and/or destabilize endosomal membranes (18–20). Antisense oligonucleotides designed to target mRNA have shown increased activity when covalently attached to or complexed with cell-penetrating peptides (21–23). For example, the 16 amino acid peptide corresponding to the third helix of the *Drosophila* homeodomain transcription

*To whom correspondence should be addressed. Tel: +1 203 737 2787; Fax: +1 203 737 2630; Email: peter.glazer@yale.edu

factor, antennapedia (Antp), has been shown to cross cell membranes and achieve intracytoplasmic and intranuclear distribution. In cell culture, an oligonucleotide–Antp conjugate produced an antisense effect by inhibiting amyloid precursor protein expression at the 40 nM level (18). However, the use of such peptides to deliver DNA-binding molecules, such as TFOs, to chromosomal sites has not been previously characterized.

With this in mind, we sought to investigate the ability of translocating peptides to enhance the intracellular delivery of TFOs. Because differences in intracellular localization have been reported among the various transport peptides, we tested Antp because it has been shown to translocate through the plasma membrane to the cytosol and nucleus of living cells (24). In the work reported here, we show that TFOs coupled to the cell-penetrating peptide, Antp, have increased intracellular activity in mammalian cells, as evaluated by the induction of chromosomal mutations in the target *supFG1* reporter gene. Confocal microscopy studies confirm intranuclear uptake, but surprisingly reveal that the base composition of the oligonucleotide cargo may affect the efficiency of peptide-mediated delivery and the pattern of intracellular distribution. Nonetheless, this work suggests that peptide conjugates may be useful reagents to increase the activity of DNA-binding molecules in cells.

MATERIALS AND METHODS

Peptides

Antp (RQIKIWFQNRRMKWKK) was synthesized by SynPep (Dublin, CA) or purchased from Qbiogene (Carlsbad, CA). The peptide was activated with a pyridyl disulfide function at its N-terminal end, to facilitate conjugation to the oligonucleotide. The peptide was high-performance liquid chromatography (HPLC) purified and analyzed by mass spectrometry.

Oligonucleotides

Oligonucleotides were synthesized by the Midland Certified Reagent Company (Midland, TX), using cyanoethyl phosphoramidite chemistry. After removal of the protecting groups by hydrolysis with concentrated ammonium hydroxide, the product was purified by reverse-phase HPLC. The ammonium salt form of the oligonucleotide was dissolved in distilled water and further purified using a NAP5 Sephadex G25 filtration column (Amersham Pharmacia Biotech). To allow coupling to the peptide, the TFO, AG30, 5′-AGG AAG GGG GGG GTG GTG GGG GAG GGG GAG $(CH_2)_3$ S-S-3′ was synthesized with a 3′-thiol group. This group was introduced by utilizing a 3′-thiol-modifier C3 CPG (Glen Research) as the solid support. The scrambled control oligonucleotide, SCR30, 5′-GGA GGA GTG GAG GGG AGT GAG GGG GGG GGG $(CH_2)_3$ S-S-3′, was synthesized using the same solid support, and used for comparison with AG30 in the mutagenesis experiments. The 3′-amino-modifier C7 CPG (Glen Research) was used to synthesize the unconjugated AG30 with a 3′-amine to prevent nuclease degradation (25). Labeled AG30 was synthesized with 5′-rhodamine and 3′-propyldisulfide modifications using rhodamine phosphoramidite and the 3′-thiol-modifier C3 S-S CPG, respectively. The labeled oligonucleotide was purified by anion-exchange HPLC. The 5′-rhodamine labeled AG30 was used in the determination of the cellular localization of the TFO–peptide conjugate. In addition, the control oligonucleotide, MIX30, 5′-AGT CAG TCA GTC AGT CAG TCA GTC AGT CAG $(CH_2)_3$ S-S-3′ was also synthesized with 5′-rhodamine and 3′-propyldisulfide modifications and used for comparison with AG30 in the microscopy and mutagenesis experiments.

The TFO, AG13, with the following sequence 5′-AGG AAG GGG GGG G $(CH_2)_3$ S-S-3′, was synthesized at Isis Pharmaceuticals (Carlsbad, CA). The TFO was synthesized using standard phosphoramidite chemistry with a 3′-thiol modifier, C3 S-S CPG (Glen Research) for peptide conjugation. Following deprotection by hydrolysis using concentrated aqueous ammonium hydroxide, the product was purified by reverse-phase HPLC. The oligonucleotide in the ammonium salt form was desalted by reverse-phase HPLC. The unconjugated AG13 was synthesized with a 3′-methoxyethyl modification at the 3′ end to ensure nuclease resistance.

Synthesis of TFO–peptide conjugates

The 3′-thiol modified TFO, AG30 (**1**; 2.38×10^{-8} moles, 236.8 μg), was dissolved in 250 μl of 0.1 M DTT and the reduction of the thiol group was allowed to proceed overnight at 37°C (Figure 1A). The solution was then applied to a NAP5 filtration column pre-equilibrated with degassed water. The reduced oligonucleotide (**3**) was eluted under gravity with 1 ml of degassed water directly into a siliconized Eppendorf tube containing a solution of activated Antp (Penetratin 1, Qbiogene) (**4**) (65 μl). If precipitation was observed, a small amount of methanol was added dropwise, and the reaction mixed by vortexing. The reaction mixture was heated at 65°C for 15 min in a tightly sealed tube, in order to eliminate the formation of secondary structures and prevent further precipitation. The reaction was incubated for an additional hour at 37°C. If required, the methanol was evaporated using a centrifugal evaporator following completion of the incubation period. The coupling reaction was monitored by means of SDS–PAGE, achieving a coupling yield of more than 95%. The overall synthetic strategy was similar to the procedure supplied by the manufacturer (Qbiogene).

The synthetic strategy used to synthesize the AG13–peptide conjugate was similar to that of the AG30–Antp, however, in this case, the oligonucleotide was activated. The deprotected 3′-thiol modified TFO, AG13 (50 OD), was dissolved in 1 ml of 0.5 M $NaHCO_3/Na_2CO_3$ buffer (pH 9), and 1 M DTT was added to give a final concentration of 0.25 M. The reduction of the thiol was allowed to proceed at room temperature for 2 h. Residual DTT was removed by RP–HPLC using a 0–40% gradient of 0.1 M NH_4OAc over 60 min in 80% CH_3CN. The purified, reduced AG13 was collected directly into a flask containing 2 mg of 2,2′-dipyridyl disulfide (Aldrich) in 500 μl of CH_3CN and 15 μl of *N*-ethyldiisopropylamine [$EtN(iPr)_2$]. After 2 h at room temperature, the reaction was concentrated in vacuum, followed by removal of excess 2,2′-dipyridyl disulfide by extraction with dichloroethane. The 3′-(2-pyridyl disulfide) derivative of AG13 was further purified by RP–HPLC. The amount of purified, activated oligonucleotide was determined spectrophotometrically.

Activated AG13 was dissolved in a degassed solution of 0.1 M KCl, 1 M urea, 0.1 M NH_4OAc, 20% acetonitrile and

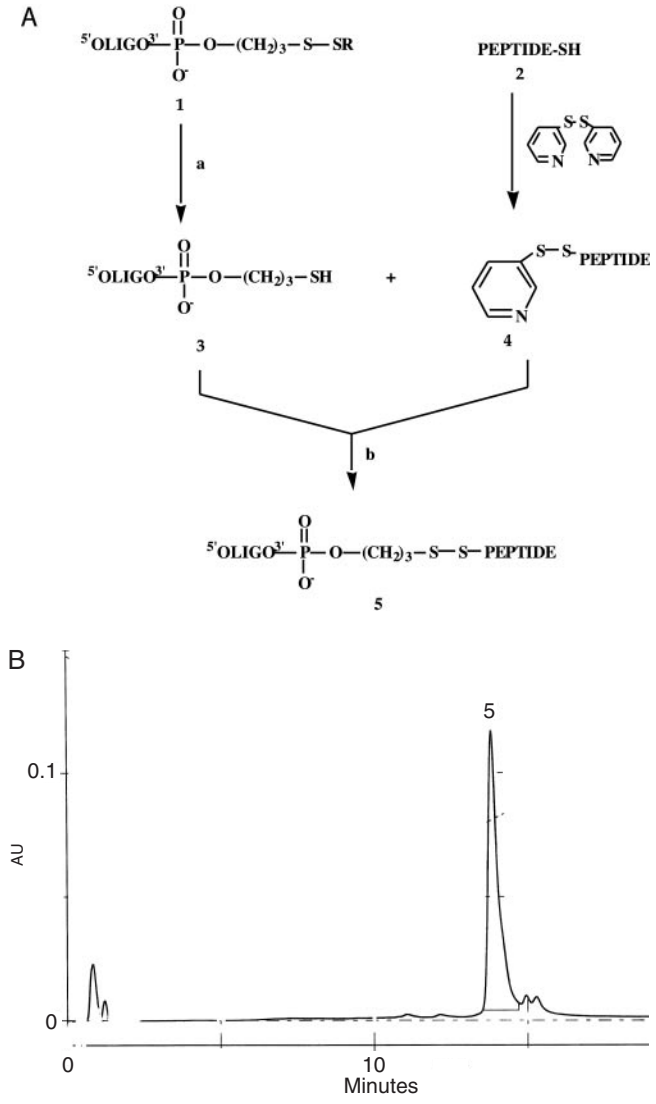

Figure 1. Preparation of a TFO–peptide conjugate. (**A**) Oligonucleotide–peptide conjugation was carried out via a disulfide linkage. The peptide was first activated with a pyridyl disulfide function at its N-terminal end to facilitate bond formation. (a) 0.1 M DTT; (b) H_2O. (**B**) HPLC analysis of TFO–peptide conjugate product.

1 μM $EtN(iPr)_2$. Under gentle mixing, Antp (10 mg), dissolved in degassed water, was added slowly to the solution of activated oligonucleotide under argon. The reaction was incubated for 2 h under argon at room temperature. The resulting conjugate was purified by ion-exchange HPLC on a Mono Q column using a 0–50% gradient of 1.5 M NaBr established over 60 min in 0.1 M NH_4OAc, 2 M urea, 30% CH_3CN. Yield 85%. The amount of AG13–Antp conjugate was determined spectrophotometrically based on molar absorption coefficients. The purity of the conjugate and verification of its composition was determined by RP–HPLC (Figure 1B) and 15% denaturing gel.

Cells and mutagenesis assay

C127 cells (CRL-1616), derived from a mammary tumor of an RIII mouse, were obtained from the American Type Culture Collection (Manassas, VA). The cells were transfected with λsupFG1 DNA using cationic lipids and selected in the presence of the neomycin analog G418 at 0.8 mg/ml (Life Technologies, Gaithersburg, MD) (26). The established cell line, AV16, containing >15 copies of the λsupFG1 shuttle vector, was maintained in medium (DMEM supplemented with 10% fetal calf serum) containing G418 at 0.8 mg/ml. Peptide conjugates were diluted (to a final concentration of 2 μM) in 2 ml of serum-free media before addition to the cells. Prior to the addition of the peptide conjugates, the cells were washed several times to eliminate the possibility of the peptide binding to dying cells and fragments of double-stranded DNA, which would lead to a reduction in the interaction with phospholipids. AV16 cells, at 70% confluence, were washed with serum-free medium, treated with the TFO–peptide mixture (or each component alone) and incubated at 37°C (Figure 2). Following a 5 h incubation, the medium volume and serum concentration were adjusted to that of normal growth conditions. The cells were collected for shuttle vector rescue and analyzed 2–4 days following treatment. Genomic DNA was isolated from the cells as described previously (27). The DNA was incubated with λ *in vitro* packing extracts for λ vector rescue from the genomic DNA and reporter gene analysis as described previously (28). Each experiment was repeated three times, and standard errors were calculated for the mutation frequency values (indicated by the error bars in the respective figures).

Microscopy

AV16 cells were plated onto glass bottom culture dishes (MatTek Corp., Ashland, MA) and grown to 70% confluency. Before addition to the cells, the rhodamine labeled oligonucleotide–peptide hybrids, AG30–Antp and MIX30–Antp, were heated at 55°C for 10 min and cooled to room temperature. After the cells were washed with serum-free media, diluted rhodamine labeled conjugate was added at a final concentration of 2 μM. For direct detection of conjugate uptake, the cells were washed extensively with serum-free media after the designated incubation period at 37°C and live cells were immediately analyzed using a Zeiss LSM 510 META confocal laser microscope (Carl Ziess Micro Imaging Inc., Thornwood, NY). Confocal microscope images of unfixed AV16 cells treated with either rhodamine labeled TFO–peptide conjugate were taken at 63× using Cy3 filter sets. For purpose of consistency, all images were focused on the nuclear membrane, with an exposure time of 1.6 s.

RESULTS

Oligonucleotide–peptide conjugates

Although complete solid-phase synthesis of oligonucleotide–peptide conjugates has been reported, side reactions during coupling cycles or cleavage from solid support tends to make this method unsuitable for the preparation of molecules in large yields (29). The major challenge for conjugation of peptides to TFOs is the incompatibility of peptide and oligonucleotide chemistry. The difficulty in solid-phase synthesis is to find compatible protecting groups for the oligonucleotide and peptide moieties. This can lead to a restriction in the choice of sequences that can be prepared. To help prevent exposure of

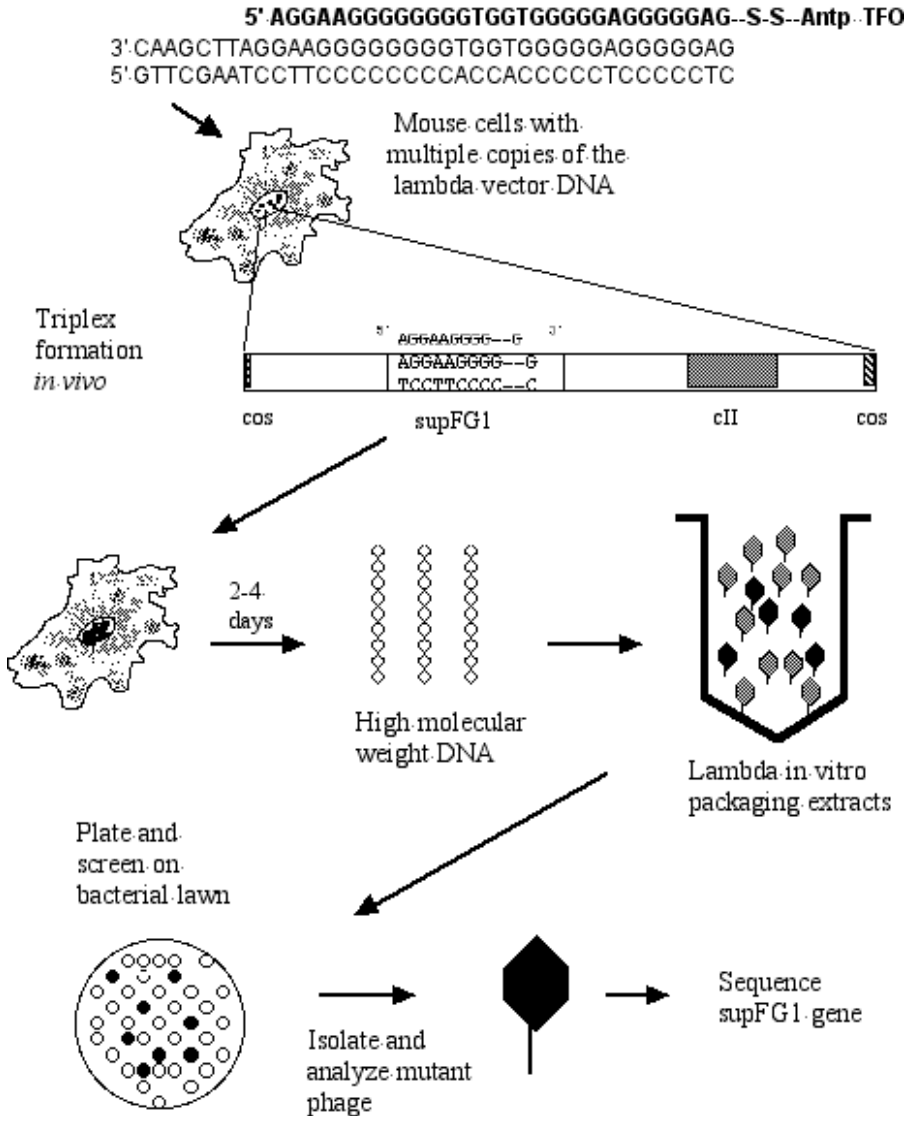

Figure 2. Experimental design for detecting chromosomal mutations induced by TFO–peptide conjugates in mouse cells. The mouse cell line, AV16, was established with multiple chromosomally integrated copies of the recoverable λ supFG1 shuttle vector carrying the *supFG1* mutation reporter gene. Following addition of the TFO–Antp conjugate (or other molecules, as described) to the medium, time is allotted for the induction of mutations before the genomic DNA is isolated and analyzed. The *supFG1* gene contains a target site where the TFO can bind as a third strand to form a triple helix. The vector DNA can be isolated, excised and packaged into viable phage for analysis in a lacZ(am) strain of *E.coli* to detect mutations that occurred in the mouse cells. If no mutation occurs in the gene, the amber mutation in the β-galactosidase gene will be suppressed and plaques will be blue in the presence of IPTG and X-Gal. However, if a mutation occurs, the amber mutation will not be suppressed and the resulting plaque will be white.

the oligonucleotide to strong acidic conditions or the peptide to strong basic conditions, post-synthetic conjugation was implemented (30,31).

We designed and synthesized TFO–Antp hybrid molecules using an overall synthetic strategy similar to that published by Vives (32). Instead of using a non-reversible linkage, such as a thioester or maleimide (33,34), we chose to use the potentially reversible disulfide bond. Such a disulfide bond may be reduced intracellularly, potentially releasing the oligonucleotide in the cytoplasm and nucleus and theoretically permitting the TFO to freely associate with the target gene (although the reducibility of the disulfide linkage in cells has not been directly established). This would eliminate the possibility of altered binding to the target site due to peptide interference. The oligonucleotide, AG30, designed to bind as a third strand to a 30 bp region of the *supFG1* gene, was synthesized using standard phosphoramidite chemistry. The 3′ end of the oligonucleotide was modified with a propyldisulfide group, while the Antp peptide was synthesized with an additional N-terminal activated cysteine residue. In addition to preventing homodimerization of the peptide, the activating pyridinium group causes the cysteine residue to become more prone to nucleophilic attack by the free sulfhydryl group on the 3′ end of the oligonucleotide. This reaction occurs rapidly at 37°C resulting in the formation of the chemically stable disulfide bond. Gel electrophoresis was used to determine purity of the conjugate. Treatment of the conjugate with excess DTT produced a shift in the gel to the original oligonucleotide. Thus, the

desired peptide conjugate was obtained using the synthetic scheme depicted in Figure 1A.

AG13–Antp was also synthesized using a disulfide bond. However, the synthetic procedure in Figure 1A was modified slightly in that the oligonucleotide 3′-thiol group was activated with a pyridinium group, instead of the peptide. However, the resulting disulfide linkage is the same. Owing to the high level of positive charges on the peptide and the negative charges of the TFO, precipitation may occur during the coupling reaction. As a result, salts and acetonitrile were used to neutralize charges and aid in solubilization. The conjugation reaction was monitored by RP–HPLC and the product purified by ion exchange HPLC (Figure 1B). RP–HPLC and 15% gel electrophoresis demonstrated high purity of the AG13–Antp conjugate. Rhodamine labeled AG30–Antp and MIX30–Antp conjugates were prepared to study the localization of the hybrid molecules in AV16 mouse cells. The labeled conjugates were synthesized using the same procedure as shown in Figure 1A.

Induced chromosomal mutations

One major obstacle in the quest to use oligonucleotides as therapeutic agents for targeted gene therapy is their limited ability to cross cell membranes. To investigate the ability of translocating peptides to improve intracellular delivery of TFOs to chromosomal sites, an assay for targeted mutagenesis in mammalian cells was used. Unlike the conventional approaches used to evaluate antisense activity, this assay does not rely on the inhibition of gene expression, where non-specific toxic effects can be confused with antisense activity. Instead, the assay has a quantitative readout for chromosomal gene targeting (Figure 2). We utilized a mouse cell line (AV16), containing multiple copies of λsupFG1 shuttle vector DNA in a chromosomal locus. The *supFG1* reporter gene contains a polypurine/polypyrimidine target site for third strand binding by either AG30 or AG13. Using packaging extracts, the vector DNA can be isolated from mouse genomic DNA into phage particles and subsequently analyzed for induced mutations (26,35,36). *SupFG1* encodes an amber suppressor tRNA whose function can be scored in indicator bacteria. A targeted mutation in the *supFG1* gene will result in the production of a white plaque upon shuttle vector rescue, in contrast to the blue plaques produced by functional *supFG1* genes. This is a useful system for evaluating the delivery of oligonucleotides to the nucleus, because site-directed mutagenesis induced by TFOs at the *supFG1* gene has been established both *in vitro* and *in vivo* (9,28).

As shown in Figure 2, the cells were incubated for 5 h with the peptide conjugates to allow cellular uptake. In order to provide an opportunity for triplex formation and mutation induction via repair and replication, the cells were harvested and the vector DNA was isolated for genetic analysis following an additional 48 h. Each experiment was repeated three times, and standard errors were calculated for the mutation frequency values. The results indicate that treatment of the cells with the TFO–peptide conjugates induced mutations at higher frequencies compared with treatment with the TFO alone (Figure 3A). The AG30–Antp hybrid molecule induced a 20-fold increase in mutation frequency when compared with direct addition of the TFO to the cell culture medium (Figure 3A). The lack of induction when AG30 and Antp

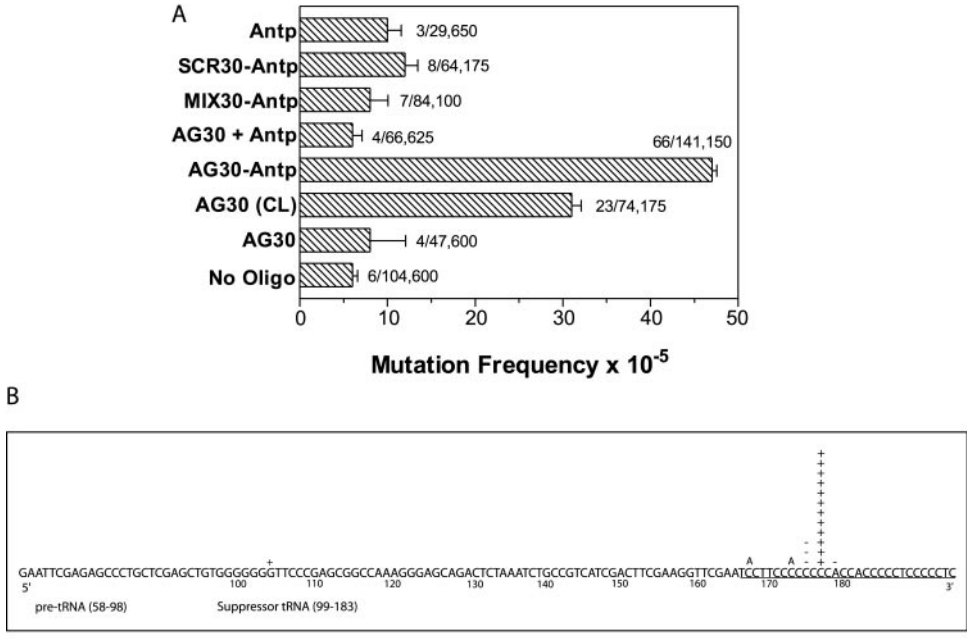

Figure 3. Targeted mutagenesis of the chromosomal *supFG1* gene in AV16 mouse cells by TFO–peptide conjugates. (**A**) Induced mutation frequencies. AG30, AG30–Antp, MIX30–Antp or Antp (2 μM final concentration) were added to the medium as indicated, and the cells were collected for DNA isolation 48 h after treatment. The frequency of mutations in the *supFG1* gene was calculated by dividing the number of colorless mutant plaques by the total number of plaques counted. AG30–Antp and MIX30–Antp indicate molecules in which the oligonucleotide was covalently linked to the peptide via a disulfide bond. The samples AG30 + Antp represent the TFO and peptide mixed together as separate unlinked molecules. CL signifies delivery via cationic lipid transfection. Each experiment was performed three times and the standard errors were calculated for the mutation frequency values, as indicated by the error bars. (**B**) Sequence analysis of the *supFG1* gene mutation induced by treatment of AV16 cells with AG30–Antp.

were simply mixed together before addition to the cell demonstrates the need for covalent linkage of the TFO to the peptide to achieve intracellular activity. Addition of Antp, by itself, to the cells did not result in induction of mutagenesis, providing evidence that the increased mutagenesis was dependent on improved TFO delivery and was not due to any peptide-induced mutations. The inability of the control oligonucleotide–peptide conjugate, MIX30–Antp, to induce mutations above background provides evidence to support a mechanism of induced mutagenesis dependent upon the binding of the TFO to its specific target site. This mechanism is further supported by the inability of the G-rich scrambled sequence control oligonucleotide–peptide conjugate, SCR30–Antp, to induce mutations above background. Transfection of AG30 using cationic lipids resulted in a mutation frequency of 31×10^{-5}, a 12-fold increase when compared to the addition of 'naked' AG30 alone to the cells. However, when the two methods of TFO transfection are compared, AG30–Antp gave mutation frequencies that were 2-fold higher than the frequency obtained when cationic lipids were used.

Sequence analysis of the AG30–Antp induced mutations revealed base substitutions and single base pair insertion and deletion mutations precisely within the TFO-binding site (Figure 3B), consistent with the previous studies (28). Because the majority of mutants analyzed were located in the triplex-binding site, the sequencing data provide further evidence that the mutations were TFO-induced and site-specific. To provide additional evidence to support a mechanism of induced mutagenesis dependent on TFO binding to a specific chromosomal target site, and to confirm specificity of gene targeting, we screened the λ *cII* gene in the same vector for possible non-specific induction of mutagenesis by the AG30–Antp peptide conjugate. The *cII* gene does not contain the TFO-binding site. In untreated AV16 cells, a background frequency of mutations in the *cII* gene of 6×10^{-5} (3/51 633) was observed (Figure 5). In cells treated with 2 μM AG30–Antp, a mutation frequency of 7×10^{-5} (6/91 800) was obtained for the *cII* gene, essentially at background. Hence, there is no non-specific mutagenic effect of the peptide conjugate in the absence of potential triplex formation. Taken together, the analysis of the pattern of mutations and the evaluation of the non-targeted *cII* gene show that the increase in mutation frequency in *supFG1* is a result of a specific and site-directed effect of the TFO–peptide conjugate and TFO binding to the *supFG1* chromosomal target site.

We also tested the ability of an Antp conjugate to increase the biological activity of a TFO with weaker binding affinity to the *supFG1* target site. AG13 was designed to bind to the first 13 bases in the 30 bp triplex-binding site in the *supFG1* gene, and binds with an affinity (equilibrium dissociation constant) of $\sim 10^{-8}$ M versus $\sim 10^{-9}$ M for AG30 (28,37). We treated AV16 mouse cells with AG13 using both peptide conjugation and cationic lipid co-mixture (Figure 4A). Conjugation of AG13 to the carrier peptide Antp resulted in a 6-fold increase in mutation frequency (30×10^{-5}) compared to direct addition of the AG13 alone to the cell culture medium. Interestingly, when transfection with cationic lipids was used, no significant increase in mutation frequency above AG13 alone was observed. Hence, the Antp conjugate conferred biological activity on AG13 that was not achieved by cationic lipid transfection. The ability of Antp conjugation to increase the effectiveness of the AG13 TFO further suggests the importance of TFO delivery in achieving bioactivity, especially with TFOs of intermediate binding affinity. The results also suggest that some polypurine sites that may be sub-optimal for TFO binding due either to reduced length or sequence inversions

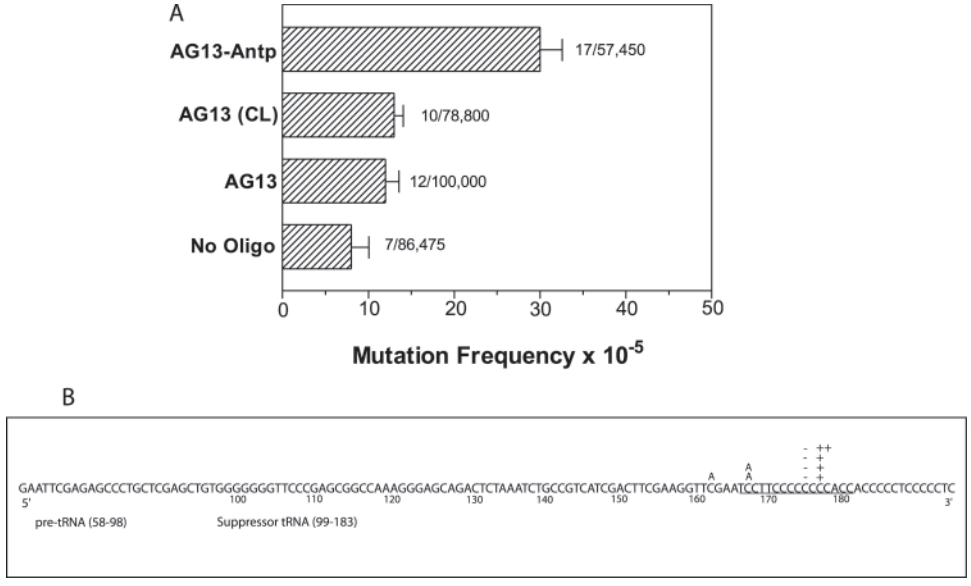

Figure 4. Targeted mutagenesis of the chromosomal *supFG1* gene in AV16 mouse cells using AG13–Antp hybrid molecules. (**A**) AG13 and AG13-peptide (2 μM final concentration) were added directly to the medium and the cells were incubated at 37°C. Cells were harvested for DNA isolation for λ vector rescue 48 h after treatment. Mutation frequency was calculated by dividing the number of colorless plaques (mutants) by the total number of plaques counted. The sample AG13–Antp indicates a molecule in which the TFO was covalently linked to the peptide. AG13 + Antp represent the TFO and peptide mixed together as separate unlinked molecules. Each experiment was performed three times and the standard errors were calculated for the mutation frequency values, as indicated by the error bars. (**B**) Sequence analysis of the *supFG1* gene mutation induced by treatment of AV16 cells with AG13–Antp.

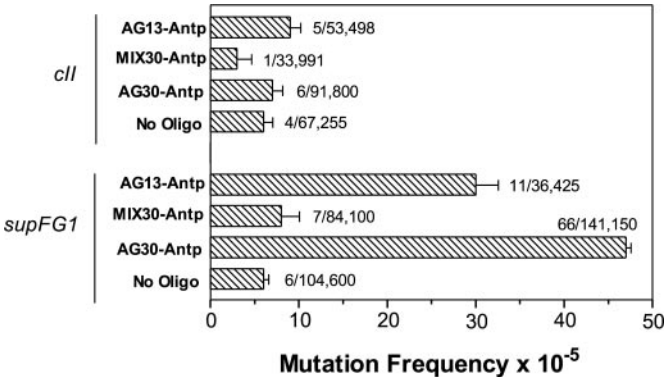

Figure 5. Comparison of targeted mutagenesis of the chromosomal *supFG1* gene and lack of TFO-induced mutagenesis of the *cII* gene in AV16 mouse cells. AG30–Antp, MIX30–Antp and AG13–Antp (2 μM) were added directly to the medium and the cells were incubated at 37°C. Cells were harvested for DNA isolation for λ vector rescue 48 h after treatment. Mutation frequency was calculated by dividing the number of colorless plaques (mutants) by the total number of plaques counted. Each experiment was performed three times and the standard errors were calculated for the mutation frequency values, as indicated by the error bars.

may still be targetable by peptide-conjugated TFOs. Sequence analysis of the AG13–Antp induced mutations also revealed base substitutions, insertions and deletions precisely within the TFO-binding site (Figure 4B). These sequencing data demonstrate that the reduced binding affinity of the TFO does not affect the specificity of gene targeting. To confirm specificity of gene targeting, we also screened the λ *cII* gene in the same vector for possible non-specific induction of mutagenesis by the AG13–Antp conjugate. In cells treated with 2 μM AG13–Antp, a mutation frequency of 9×10^{-5}, was obtained essentially at background (Figure 5). As a result, one can conclude that the increase in mutagenesis observed with the AG13–Antp conjugate can be attributed to improved delivery.

To investigate further the ability of the peptide to improve the biological activity of TFOs, dose–response experiments were performed (Tables 1 and 2). The results reveal that the induced mutation frequency increased with increasing concentrations of the AG30–Antp conjugate (Table 1). A mutation frequency of 47×10^{-5} was observed when AV16 cells were treated with 0.1 μM of AG30–Antp, while a frequency of 86×10^{-5} was obtained with an increased concentration of 5 μM. Similar results were observed in the case of AG13–Antp (Table 2). As the concentration of conjugate administered increased, an increase in mutation frequency was noted, ranging from 24×10^{-5} to 58×10^{-5} with treatments of 0.1–5 μM, respectively.

Table 1. Dose dependence of AG30–Antp peptide conjugate on the frequency of induced chromosomal mutations in *supFG1* gene in AV16 mouse cells

Concentration (μM)	Mutants/total plaques	Mutation frequency (10^{-5})
None	11/60 975	18
0.1	59/125 825	47
0.5	41/72 850	56
1.0	47/73 100	64
2.0	44/56 875	77
5.0	53/61 350	86
Antp*	5/64 325	8

The frequency of mutations in the *supFG1* gene was calculated by dividing the number of clear mutant plaques by the total number of plaques counted. Asterisk indicates Antp peptide by itself at 10 μM in the absence of TFO.

Table 2. Dose dependence of targeted mutagenesis of the chromosomal *supFG1* gene in AV16 mouse cells by AG13–Antp peptide conjugate

Concentration (μM)	Mutants/total plaques	Mutation frequency (10^{-5})
None	13/88 350	15
0.1	12/49 875	24
0.5	19/54 950	35
1.0	25/54 900	45
2.0	40/73 125	55
5.0	39/66 750	58

The frequency of mutations in the *supFG1* gene was calculated by dividing the number of clear mutant plaques by the total number of plaques counted.

Microscopy

It has been shown that peptides bind strongly to the cell membrane and remain associated with cells even after repeated washings. As a result, FACS analysis cannot be reliably used to evaluate uptake unless a protease digestion step of the adsorbed proteins is included in the protocol (38). Cellular uptake of the AG30–Antp conjugate was instead evaluated using confocal microscopy. Because it has been demonstrated that cell fixation, even under mild conditions, leads to the artifactual uptake of transport peptides (38), we chose to perform microscopy on live unfixed cells. This technique allowed us to visually demonstrate a difference in the uptake of labeled-TFO and labeled TFO–Antp.

The rhodamine-labeled AG30–Antp and the rhodamine-labeled AG30 were incubated with AV16 cells at 37°C for periods of 5 and 24 h, after which the cells were examined by confocal microscopy. Surprisingly, rhod–AG30 exhibited significantly more uptake than would be expected by passive diffusion, with uneven distribution of the oligonucleotide throughout the cell (Figure 6A). The majority of the fluorescence is observed in the cytoplasm, with punctate distribution in the area surrounding the nucleus. However, there was some detectable uptake into the nucleus. The intensity of fluorescence did not increase with time. In fact, after 24 h, there was an apparent decrease in the intensity of punctate foci in the area surrounding the nucleus (Figure 6B) Rhodamine–AG30 was also transfected into the cell using cationic lipids. This method of transfection resulted in punctate distribution of fluorescence in the area surrounding the nucleus, with negligible staining of the nucleus (Figure 6C). After 24 h, the intensity of the rhodamine increased, but there was still no significant uptake in the nucleus (Figure 6D).

The AG30–Antp conjugate was more evenly distributed within the cells, with less difference between the nucleus and cytoplasm (Figure 6E). Both diffuse and punctate cytoplasmic fluorescence was observed. After 24 h, the accumulation of labeled AG30–Antp increased, with higher levels of punctate cytoplasmic fluorescence (Figure 6F). Some fluorescence was observed on the cell surface, which can be attributed to the accumulation of oligonucleotide–peptide conjugate. This may be caused by the formation of secondary structures, due to the G-rich content of AG30. (The conjugate was heated at 55°C for 5 min before use in uptake experiments to try to

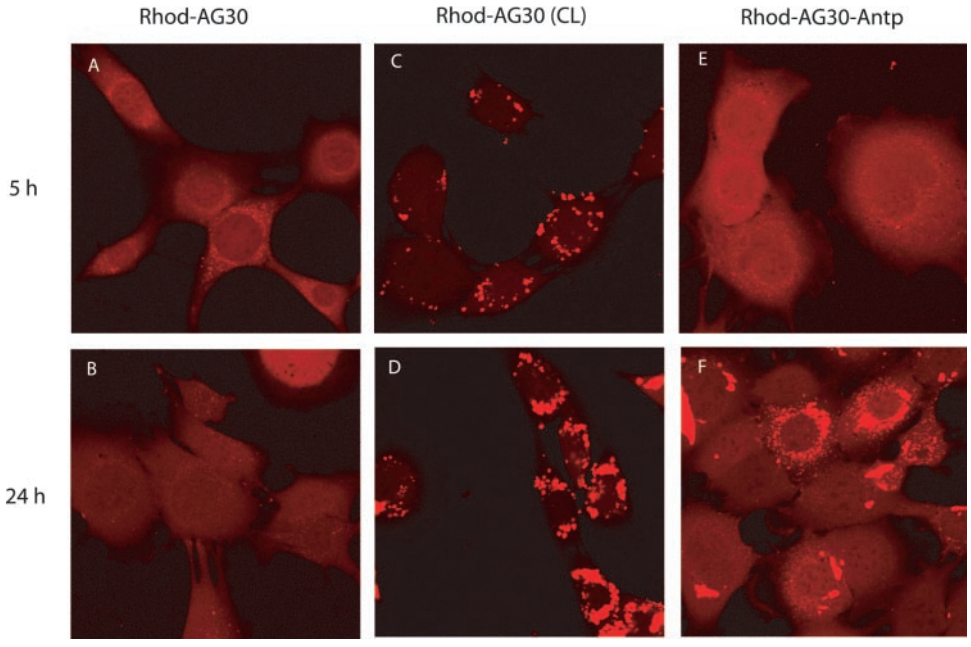

Figure 6. Internalization of rhodamine-labeled AG30–Antp conjugate by AV16 mouse cells. Cells were incubated with either rhodamine–AG30 (**A** and **B**), rhodamine–AG30 mixed with cationic lipids (CL) (**C** and **D**) or rhodamine–AG30–Antp (**E** and **F**) at a concentration of 2 μM for 5 or 24 h. Unfixed cells were examined by confocal microscopy.

minimize this phenomenon.) Overall, comparison of the images reveals that the rhodamine signal accumulated in the cells to varying extents in all cases. However, the intensity of intracellular fluorescence is greater for the AG30–Antp conjugate than for the oligonucleotide alone. In addition, the rhodamine-labeled AG30–Antp conjugate showed a less punctate and more diffuse cellular distribution than did the rhodamine-labeled unconjugated AG30.

Nonetheless, the uptake of AG30 without the aid of any special transfection method beyond addition to the culture medium is noteworthy. Other microscopy based analyses of oligonucleotide uptake have revealed minimal uptake in the absence of transfection (39). To investigate whether the uptake observed with AG30 might be due to its G-rich content, a rhodamine-labeled oligonucleotide with a balanced base composition, MIX30, was incubated with AV16 cells for 5 h. Uptake of MIX30 was examined using confocal microscopy, and no detectable intracellular fluorescence was observed (Figure 7A), consistent with other published reports (30,40). Some uptake of rhod–MIX30 was eventually detectable after 24 h (Figure 7B), but at intensities similar to what was observed with rhod–AG30 after only 5 h (Figure 6B). The distribution of uptake in the case of MIX30 at 24 h was also punctate in the region surrounding the nucleus, suggesting endocytosis as a possible mechanism of uptake. In contrast, when rhod–MIX30 was conjugated to Antp and incubated for 5 h with AV16 cells, there was substantial cellular uptake, even more than the AG30–Antp conjugate (Figure 7C). In addition, the distribution of rhod–MIX30 within the cells was mostly nuclear, with lesser intensity in the cytoplasm (Figure 7C). After a 24 h incubation period, the fluorescence distribution was the same (Figure 7D). Hence, although Antp conjugation enhanced the overall cellular uptake of both AG30 and MIX30, a much higher proportion of intranuclear uptake

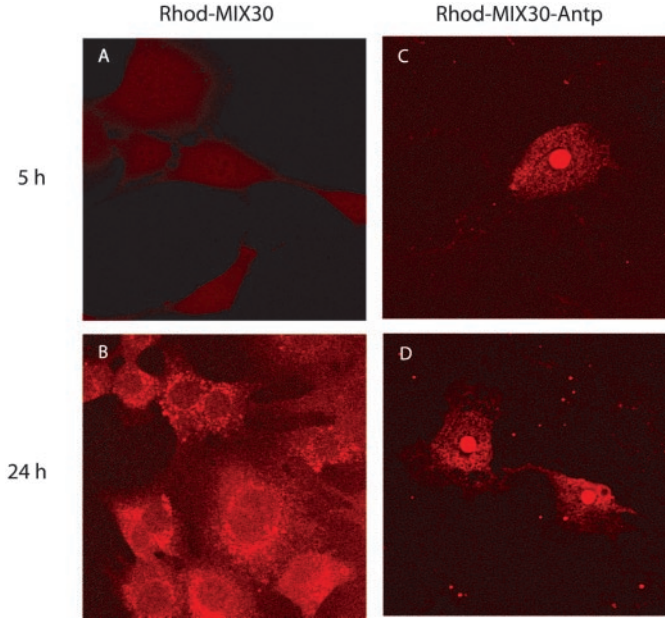

Figure 7. Internalization of rhodamine labeled MIX30–Antp conjugate in AV16 mouse cells. Cells were incubated with either rhodamine–MIX30 (**A** and **B**) or rhodamine MIX30–Antp (**C** and **D**) for 5 or 24 h, as indicated and examined by confocal microscopy without prior fixation.

was achieved with MIX30. These studies suggest that the characteristics of the oligonucleotide cargo linked to a cell-penetrating peptide can affect the efficiency of intracellular delivery and the pattern of intracellular distribution. However, one caveat to keep in mind is that this cargo-dependent effect was observed in just one cell line (AV16), and may not be generalizable to all cell lines.

DISCUSSION

Delivery of a TFO to its chromosomal target is critical to its biological efficacy. Therefore, an important goal is enhancement of transmembrane penetration and localization to the intranuclear compartment containing the target gene. A 16-amino acid peptide corresponding to the third helix of the homeodomain of the *Drosophila* Antp transcription factor was used to deliver covalently attached TFOs into mouse cells. Treatment of cells with the AG30–Antp conjugate increased the mutation frequency of the *supFG1* reporter gene by 20-fold when compared to direct addition of 'naked' oligonucleotide. Antp conjugation also enhanced the biological activity of AG13, a TFO with a lower binding affinity for the target gene, resulting in an induced mutation frequency above background that was otherwise not observed even when cationic lipids were used for transfection.

The mechanism of internalization of translocating peptides and their cargo is not well understood and has been the subject of much controversy. Several reports in the literature indicate that cellular uptake by cationic cell penetrating peptides proceeds via an energy independent mechanism and does not involve endocytosis, thus delivering cargo directly to the cytoplasm and allowing free diffusion into the nucleus of the cell. One proposed model suggests that the peptides interact with charged phospholipids on the outside of the membrane. This results in destabilization of the bilayer and formation of inverted micelles that travel across the membrane and subsequently release the cargo in the cytoplasmic compartment (41). However, other studies suggest the involvement of endocytosis in the internalization of cell penetrating peptides (38,42,43), a situation that would restrict intracellular trafficking. We cannot exclude the possibility that a small fraction of the oligonucleotide–peptide conjugate enters the cell by an endocytosis-dependent pathway. However, at least some portion of the TFO delivery can be inferred to be nuclear, since mutagenesis of the target *supFG1* gene is certainly a nuclear event.

The microscopy studies show that Antp conjugation yields enhanced intracellular uptake of AG30, consistent with the results of the targeted mutagenesis assay. However, there are two additional observations of note. One is that AG30, by itself, showed some detectable intracellular uptake. This is consistent with biological evidence for the uptake of psoralen-linked AG30 (based on mutagenesis assays) in some of our previous studies using other cell types (28). However, it is generally thought that standard diester oligonucleotides are poorly taken up by cells. It may be that the G-rich nature of AG30 enhances uptake, since the MIX30 oligonucleotide showed less uptake in the absence of Antp conjugation, consistent with other studies of oligonucleotide uptake. The second point is that, conversely, the extent of intranuclear accumulation of AG30 with Antp-mediated delivery was not as great as that of MIX30 under the same conditions. AG30 has 23 Gs, 5 As and 2 Ts, whereas MIX30 has 8 Gs, 8 As, 7 Ts and 7 Cs. Hence, it is possible that the base composition of the cargo oligonucleotide can influence the efficiency of uptake or the pattern of intracellular distribution following transmembrane delivery. It may be that the G-rich nature of AG30 promotes secondary structure formation, including intra- and intermolecular G-quartets (44,45). G-rich oligonucleotides have also been reported to form homodimers (46). Such structures may influence intracellular localization and trafficking, possibly by interaction with cellular proteins with affinity for non-conical DNA structures (47). A systematic analysis of the sequence dependence of oligonucleotide intracellular uptake and localization will be needed to further investigate these possibilities.

Nonetheless, the work reported here demonstrates that the use of carrier peptides to increase the cellular uptake of TFOs in cells is a potentially powerful tool. Such peptides offer several advantages including low toxicity and internalization by most cells. Additional modifications to further enhance the bioactivity of the TFO–peptide conjugates are also possible. For example, it might be advantageous to conjugate TFOs to peptide sequences that could provide both cell membrane transport and nuclear transport, since direct trafficking of oligonucleotide–peptide conjugates to nuclei may result in even greater chromosomal gene targeting. In one report, an NLS peptide conjugated to an ^{125}I-labeled TFO provided improved activity in cells (48). Other types of peptide sequences may provide additional advantages beyond improved uptake and intranuclear delivery, such as improved DNA binding and triplex formation under physiological conditions. In this regard, it may turn out to be advantageous to generate a covalent TFO–peptide linkage via a non-reducible bond to take advantage of the ability of a peptide conjugate to enhance DNA binding. In any case, the results here demonstrate that selected peptides can facilitate TFO-mediated gene targeting and provide the basis for future efforts to use peptide conjugates to enhance the bioactivity of molecules designed to target chromosomal DNA.

ACKNOWLEDGEMENTS

We thank L. Narayanan, A. Gustav, D. Campisi, E. Kosowsky, P. Male and L. Cabral for their help. This work was supported by the National Institutes of Health (R01CA64186 and R01GM54731) to P.M.G., and F.A.R. was supported by institutional NRSA awards from the National Institutes of Health (T32CA09259 and T32CA09159) and by a fellowship from the Lucille B. Markey Charitable Trust.

REFERENCES

1. Giovannangeli,C. and Helene,C. (2000) Triplex-forming molecules for modulation of DNA information processing. *Curr. Opin Mol. Ther.*, **2**, 288–296.
2. Knauert,M.P. and Glazer,P.M. (2001) Triplex forming oligonucleotides: sequence-specific tools for gene targeting. *Hum. Mol. Genet.*, **10**, 2243–2251.
3. Faria,M., Wood,C.D., Perrouault,L., Nelson,J.S., Winter,A., White,M.R., Helene,C. and Giovannangeli,C. (2000) Targeted inhibition of transcription elongation in cells mediated by triplex-forming oligonucleotides. *Proc. Natl Acad. Sci. USA*, **97**, 3862–3867.
4. Takasugi,M., Guendouz,A., Chassignol,M., Decout,J.L., Lhomme,J., Thuong,N.T. and Helene,C. (1991) Sequence-specific photo-induced cross-linking of the two strands of double-helical DNA by a psoralen covalently linked to a triple helix-forming oligonucleotide. *Proc. Natl Acad. Sci. USA*, **88**, 5602–5606.
5. Havre,P.A., Gunther,E.J., Gasparro,F.P. and Glazer,P.M. (1993) Targeted mutagenesis of DNA using triple helix-forming oligonucleotides linked to psoralen. *Proc. Natl Acad. Sci. USA*, **90**, 7879–7883.

6. Wang,G., Seidman,M.M. and Glazer,P.M. (1996) Mutagenesis in mammalian cells induced by triple helix formation and transcription-coupled repair. *Science*, **271**, 802–805.
7. Vasquez,K.M., Wensel,T.G., Hogan,M.E. and Wilson,J.H. (1996) High-efficiency triple-helix-mediated photo-cross-linking at a targeted site within a selectable mammalian gene. *Biochemistry*, **35**, 10712–10719.
8. Wang,X., Tolstonog,G., Shoeman,R.L. and Traub,P. (1996) Selective binding of specific mouse genomic DNA fragments by mouse vimentin filaments *in vitro*. *DNA Cell Biol.*, **15**, 209–225.
9. Vasquez,K.M., Narayanan,L. and Glazer,P.M. (2000) Specific mutations induced by triplex-forming oligonucleotides in mice. *Science*, **290**, 530–533.
10. Chan,P.P., Lin,M., Faruqi,A.F., Powell,J., Seidman,M.M. and Glazer,P.M. (1999) Targeted correction of an episomal gene in mammalian cells by a short DNA fragment tethered to a triplex-forming oligonucleotide. *J. Biol. Chem.*, **274**, 11541–11548.
11. Luo,Z., Macris,M.A., Faruqi,A.F. and Glazer,P.M. (2000) High-frequency intrachromosomal gene conversion induced by triplex-forming oligonucleotides microinjected into mouse cells. *Proc. Natl Acad. Sci. USA*, **97**, 9003–9008.
12. Datta,H.J., Chan,P.P., Vasquez,K.M., Gupta,R.C. and Glazer,P.M. (2001) Triplex-induced recombination in human cell-free extracts. Dependence on XPA and HsRad51. *J. Biol. Chem.*, **276**, 18018–18023.
13. Yakubov,L.A., Deeva,E.A., Zarytova,V.F., Ivanova,E.M., Ryte,A.S., Yurchenko,L.V. and Vlassov,V.V. (1989) Mechanism of oligonucleotide uptake by cells: involvement of specific receptors? *Proc. Natl Acad. Sci. USA*, **86**, 6454–6458.
14. Harris,J.D. and Lemoine,N.R. (1996) Strategies for targeted gene therapy. *Trends Genet.*, **12**, 400–405.
15. Stein,C.A. and Cheng,Y.C. (1993) Antisense oligonucleotides as therapeutic agents—is the bullet really magical? *Science*, **261**, 1004–1012.
16. Felgner,J.H., Kumar,R., Sridhar,C.N., Wheeler,C.J., Tsai,Y.J., Border,R., Ramsey,P., Martin,M. and Felgner,P.L. (1994) Enhanced gene delivery and mechanism studies with a novel series of cationic lipid formulations. *J. Biol. Chem.*, **269**, 2550–2561.
17. Lewis,J.G., Lin,K.Y., Kothavale,A., Flanagan,W.M., Matteucci,M.D., DePrince,R.B., Mook,R.A.,Jr, Hendren,R.W. and Wagner,R.W. (1996) A serum-resistant cytofectin for cellular delivery of antisense oligodeoxynucleotides and plasmid DNA. *Proc. Natl Acad. Sci. USA*, **93**, 3176–3181.
18. Allinquant,B., Hantraye,P., Mailleux,P., Moya,K., Bouillot,C. and Prochiantz,A. (1995) Downregulation of amyloid precursor protein inhibits neurite outgrowth *in vitro*. *J. Cell Biol.*, **128**, 919–927.
19. Vives,E., Brodin,P. and Lebleu,B. (1997) A truncated HIV-1 Tat protein basic domain rapidly translocates through the plasma membrane and accumulates in the cell nucleus. *J. Biol. Chem.*, **272**, 16010–16017.
20. Bongartz,J.P., Aubertin,A.M., Milhaud,P.G. and Lebleu,B. (1994) Improved biological activity of antisense oligonucleotides conjugated to a fusogenic peptide. *Nucleic Acids Res.*, **22**, 4681–4688.
21. Lindgren,M., Hallbrink,M., Prochiantz,A. and Langel,U. (2000) Cell-penetrating peptides. *Trends Pharmacol. Sci.*, **21**, 99–103.
22. Prochiantz,A. (1996) Getting hydrophilic compounds into cells: lessons from homeopeptides. *Curr. Opin. Neurobiol.*, **6**, 629–634.
23. Astriab-Fisher,A., Sergueev,D.S., Fisher,M., Shaw,B.R. and Juliano,R.L. (2000) Antisense inhibition of P-glycoprotein expression using peptide–oligonucleotide conjugates. *Biochem. Pharmacol.*, **60**, 83–90.
24. Derossi,D., Joliot,A.H., Chassaing,G. and Prochiantz,A. (1994) The third helix of the Antennapedia homeodomain translocates through biological membranes. *J. Biol. Chem.*, **269**, 10444–10450.
25. Zendegui,J.G., Vasquez,K.M., Tinsley,J.H., Kessler,D.J. and Hogan,M.E. (1992) *In vivo* stability and kinetics of absorption and disposition of 3′ phosphopropyl amine oligonucleotides. *Nucleic Acids Res.*, **20**, 307–314.
26. Glazer,P.M., Sarkar,S.N. and Summers,W.C. (1986) Detection and analysis of UV-induced mutations in mammalian cell DNA using a lambda phage shuttle vector. *Proc. Natl Acad. Sci. USA*, **83**, 1041–1044.
27. Gunther,E.J., Yeasky,T.M., Gasparro,F.P. and Glazer,P.M. (1995) Mutagenesis by 8-methoxypsoralen and 5-methylangelicin photoadducts in mouse fibroblasts: mutations at cross-linkable sites induced by monoadducts as well as cross-links. *Cancer Res.*, **55**, 1283–1288.
28. Vasquez,K.M., Wang,G., Havre,P.A. and Glazer,P.M. (1999) Chromosomal mutations induced by triplex-forming oligonucleotides in mammalian cells. *Nucleic Acids Res.*, **27**, 1176–1181.
29. Tung,C.H. and Stein,S. (2000) Preparation and applications of peptide–oligonucleotide conjugates. *Bioconjug. Chem.*, **11**, 605–618.
30. Antopolsky,M., Azhayeva,E., Tengvall,U., Auriola,S., Jaaskelainen,I., Ronkko,S., Honkakoski,P., Urtti,A., Lonnberg,H. and Azhayev,A. (1999) Peptide–oligonucleotide phosphorothioate conjugates with membrane translocation and nuclear localization properties. *Bioconjug. Chem.*, **10**, 598–606.
31. Chen,C.P., Zhang,L.R., Peng,Y.F., Wang,X.B., Wang,S.Q. and Zhang,L.H. (2003) A concise method for the preparation of peptide and arginine-rich peptide-conjugated antisense oligonucleotide. *Bioconjug. Chem.*, **14**, 532–538.
32. Vives,E. and Lebleu,B. (1997) Selective coupling of a highly basic peptide to an oligonucleotide. *Tetrahedron Lett.*, **38**, 1183–1186.
33. Zhu,T., Wei,Z., Tung,C.H., Dickerhof,W.A., Breslauer,K.J., Georgopoulos,D.E., Leibowitz,M.J. and Stein,S. (1993) Oligonucleotide-poly-L-ornithine conjugates: binding to complementary DNA and RNA. *Antisense Res. Dev.*, **3**, 265–275.
34. Ede,N.J., Tregear,G.W. and Haralambidis,J. (1994) Routine preparation of thiol oligonucleotides: application to the synthesis of oligonucleotide–peptide hybrids. *Bioconjug. Chem.*, **5**, 373–378.
35. Narayanan,L., Fritzell,J.A., Baker,S.M., Liskay,R.M. and Glazer,P.M. (1997) Elevated levels of mutation in multiple tissues of mice deficient in the DNA mismatch repair gene Pms2. *Proc. Natl Acad. Sci. USA*, **94**, 3122–3127.
36. Gunther,E.J., Murray,N.E. and Glazer,P.M. (1993) High efficiency, restriction-deficient *in vitro* packaging extracts for bacteriophage lambda DNA using a new *E.coli* lysogen. *Nucleic Acids Res.*, **21**, 3903–3904.
37. Faruqi,A.F., Krawczyk,S.H., Matteucci,M.D. and Glazer,P.M. (1997) Potassium-resistant triple helix formation and improved intracellular gene targeting by oligodeoxyribonucleotides containing 7-deazaxanthine. *Nucleic Acids Res.*, **25**, 633–640.
38. Richard,J.P., Melikov,K., Vives,E., Ramos,C., Verbeure,B., Gait,M.J., Chernomordik,L.V. and Lebleu,B. (2003) Cell-penetrating peptides. A reevaluation of the mechanism of cellular uptake. *J. Biol. Chem.*, **278**, 585–590.
39. Hope,M.J., Mui,B., Ansell,S. and Ahkong,Q.F. (1998) Cationic lipids, phosphatidylethanolamine and the intracellular delivery of polymeric, nucleic acid-based drugs (review). *Mol. Membr. Biol.*, **15**, 1–14.
40. Dom,G., Shaw-Jackson,C., Matis,C., Bouffioux,O., Picard,J.J., Prochiantz,A., Mingeot-Leclercq,M.P., Brasseur,R. and Rezsohazy,R. (2003) Cellular uptake of Antennapedia Penetratin peptides is a two-step process in which phase transfer precedes a tryptophan-dependent translocation. *Nucleic Acids Res.*, **31**, 556–561.
41. Derossi,D., Chassaing,G. and Prochiantz,A. (1998) Trojan peptides: the penetratin system for intracellular delivery. *Trends Cell Biol.*, **8**, 84–87.
42. Thoren,P.E., Persson,D., Isakson,P., Goksor,M., Onfelt,A. and Norden,B. (2003) Uptake of analogs of penetratin, Tat(48–60) and oligoarginine in live cells. *Biochem. Biophys. Res. Commun.*, **307**, 100–107.
43. Letoha,T., Gaal,S., Somlai,C., Czajlik,A., Perczel,A. and Penke,B. (2003) Membrane translocation of penetratin and its derivatives in different cell lines. *J. Mol. Recognit.*, **16**, 272–279.
44. Cheng,A.J. and Van Dyke,M.W. (1997) Oligodeoxyribonucleotide length and sequence effects on intramolecular and intermolecular G-quartet formation. *Gene*, **197**, 253–260.
45. Cheng,A.J., Wang,J.C. and Van Dyke,M.W. (1998) Self-association of G-rich oligodeoxyribonucleotides under conditions promoting purine-motif triplex formation. *Antisense Nucleic Acid Drug Dev.*, **8**, 215–225.
46. Noonberg,S.B., Francois,J.C., Garestier,T. and Helene,C. (1995) Effect of competing self-structure on triplex formation with purine-rich oligodeoxynucleotides containing GA repeats. *Nucleic Acids Res.*, **23**, 1956–1963.
47. Bates,P.J., Kahlon,J.B., Thomas,S.D., Trent,J.O. and Miller,D.M. (1999) Antiproliferative activity of G-rich oligonucleotides correlates with protein binding. *J. Biol Chem.*, **274**, 26369–26377.
48. Sedelnikova,O.A., Karamychev,V.N., Panyutin,I.G. and Neumann,R.D. (2002) Sequence-specific gene cleavage in intact mammalian cells by 125I-labeled triplex-forming oligonucleotides conjugated with nuclear localization signal peptide. *Antisense Nucleic Acid Drug Dev.*, **12**, 43–49.